

Naphtho[1,2-*b*:5,6-*b'*]dithiophene-Based Small Molecules for Thick-Film Organic Solar Cells with High Fill Factors

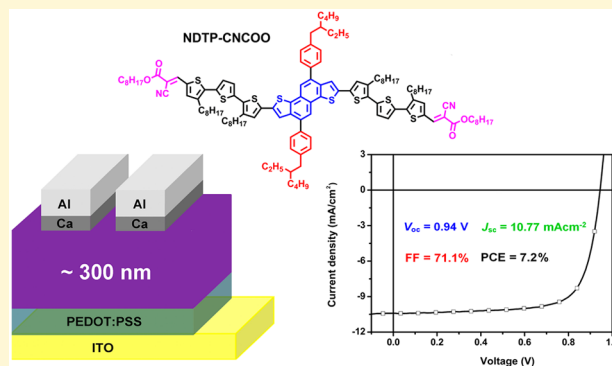
Xiangwei Zhu,^{†,‡} Benzheng Xia,[†] Kun Lu,^{*,†} Huan Li,[†] Ruimin Zhou,[†] Jianqi Zhang,[†] Yajie Zhang,[†] Zhigang Shuai,[‡] and Zhixiang Wei^{*,†}

[†]National Center for Nanoscience and Technology, Beijing, 100190, P. R. China

[‡]Department of Chemistry, Tsinghua University, Beijing, 100084, P. R. China

S Supporting Information

ABSTRACT: Two novel acceptor–donor–acceptor type small molecules based on a two-dimensional conjugated naphtho[1,2-*b*:5,6-*b'*]dithiophene (NDT) unit containing alkylthienyl or alkylphenyl side chains, named as NDTT-CNCOO and NDTP-CNCOO, respectively, were designed and synthesized. Compared with NDTT-CNCOO, NDTP-CNCOO-based bulk heterojunction (BHJ) solar cells exhibited higher fill factors, higher short current density, and higher power conversion efficiencies. Such performance benefitted from highly ordered structures, excellent charge transport property, and good film formation capability. The fill factors of BHJ solar cells using NDTP-CNCOO as a donor and [6,6]-phenyl-C71-butyric acid methyl ester (PC₇₁BM) as an acceptor were all above 70% with thicknesses of active layers ranging from 100 to 300 nm. In particular, the optimal power conversion efficiency of the solar cell devices reached 7.20% with an active layer thickness of 300 nm, which is the best result reported for NDT-based small molecule solar cells.



INTRODUCTION

Conjugated small molecules with acceptor–donor–acceptor (A–D–A) structures are promising materials for bulk heterojunction (BHJ) organic solar cells (OSCs).¹ The power conversion efficiency (PCE) of this type of small molecule, typically using oligothiophenes or benzo[1,2-*b*:4,5-*b'*]dithiophene (BDT) as the donor core,^{2,3} has reached ca. 10% by optimizing their molecular structure and device fabrication conditions.^{4,5} However, their optimized devices are mostly obtained at ca. 100 nm thick active layers, which are not preferable for large-scale printing technology. Consequently, a series of highly efficient donor materials with optimal performances that can be obtained using films with a thickness of over 200 nm must be developed.⁶ To date, various donor materials with an optimal active layer thickness of ~300 nm have been reported, but most of these materials are polymer donors.^{7–12} Compared with polymer donors, only a few examples on small molecule-based devices with PCE higher than 7% have been reported using thick films (>200 nm).^{13–15} Thus, the design and synthesis of high-performance small molecules being used in thick film are of great importance for large-area OSCs through solution-processing techniques.

To obtain a material with good photovoltaic performance using thick active layers, an effective technique is one that improves the charge transport ability to overcome the enhanced charge recombination because of the increase in carrier drift length.¹⁶ Notably, donor materials with highly ordered

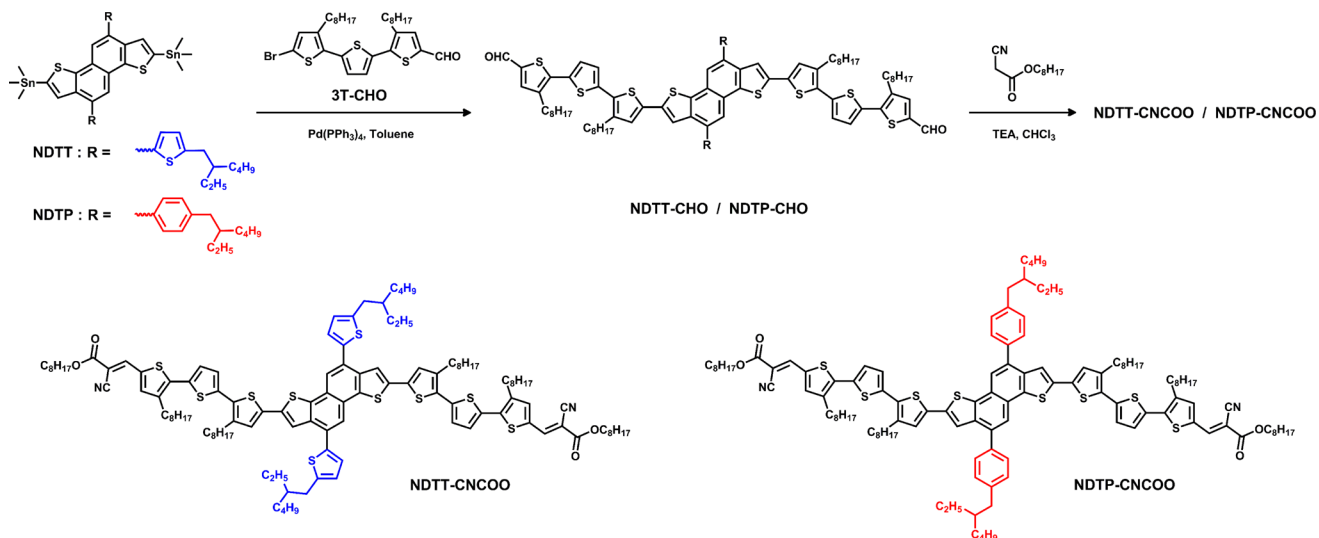
structures are expected to achieve high hole mobility.¹⁷ Compared with polymers, small molecules may form much higher-order structures as they possess superior crystallization capability. However, for a majority of small molecules, much stronger crystallinity often leads to large-scale aggregation of both donor and acceptor phases, which restrict charge carrier transport in both phases. Thus, the photovoltaic performances of small molecules decrease significantly with thick active layers. To overcome the above-mentioned limitation, a balance between crystallinity and phase separation must be established. In our previous work, we have proved that a two-dimensional (2D)-conjugated naphtho[1,2-*b*:5,6-*b'*]dithiophene (NDT) unit, which attaches alkylthienyl conjugated side chains on its own core, is an excellent potential candidate unit for the design and construction of highly efficient thick-film polymer photovoltaic materials. Such a structure can effectively expand the conjugating surface, enhance the intermolecular π – π interactions, and facilitate charge transport. Moreover, we also found that altering the molecular structure is a highly effective approach to control the molecular stacking mode and active layer morphology.¹⁸ Thus, the application of the 2D-conjugated NDT unit to the small molecule system may result in a novel type of highly efficient photovoltaic material, with a

Received: December 2, 2015

Revised: January 20, 2016

Published: January 20, 2016

Scheme 1. Synthetic Routes of NDTT-CNCOO and NDTP-CNCOO



corresponding device performance that is relatively independent of the film thickness of the active layers. Previously reported NDT-based small molecules with alkoxy side chains have less than 5% PCE.^{19–21} 2D-conjugated NDT unit-based small molecules are also expected to exhibit extended absorption spectra, high hole mobility, and enhanced photovoltaic performances compared with those using alkoxy-substituted NDT as core.

In this work, two novel small molecules (NDTT-CNCOO and NDTP-CNCOO) based on the 2D-conjugated NDT unit were designed and synthesized (Scheme 1). However, the crystallinity of NDTT-CNCOO was so strong that the NDTT-CNCOO/[6,6]-phenyl-C₇₁-butyric acid methyl ester (PC₇₁BM) blend film displayed large domains and a high level of aggregation, leading to poor device performance. Therefore, to obtain high photovoltaic performance, tuning the aggregation behavior of small molecules and the optimization of the morphology of blend films are essential. Altering the side chains of small molecules is an effective strategy to modify the morphology of the active layer. A weak electron-donating unit, alkylphenyl side chain, was therefore introduced into the NDT core instead of the alkylthienyl part, as this approach could change the intermolecular π - π interactions to some extent and lower the highest occupied molecular orbital (HOMO) level of the conjugated system, boosting the open-circuit voltage (V_{oc}).^{22–24} Finally, the modified small molecule (NDTP-CNCOO) exhibited a highly ordered structure and proper scale phase separation after blending with PC₇₁BM, which facilitated the charge carrier separation and transport, leading to higher fill factor (FF) and PCE for the NDTP-CNCOO/PC₇₁BM-based BHJ solar cells even with thick active layers (thicker than 200 nm). More importantly, the device performances were all above 6.0% with thicknesses of active layers ranging from 200 to 400 nm. The best PCE reached 7.20%, and the FF exceeded 70% with an active layer thickness of 300 nm, which is the best result reported for NDT-based small molecule BHJ solar cells to date. Such an outstanding photovoltaic property of NDTP-CNCOO indicated that 2D-conjugated NDT-based small molecules are highly promising candidates for manufacturing high-performance, large-area BHJ solar cells through solution-processing techniques.

RESULTS AND DISCUSSION

The synthetic routes of NDTT-CNCOO and NDTP-CNCOO are shown in Scheme 1. NDTT, NDTP, and 3T-CHO were prepared by a similar method reported in previous studies.^{25,26} NDTT, NDTP, and 3T-CHO were then programmed to synthesize the intermediates (NDTT-CHO and NDTP-CHO) by the Stille cross-coupling reaction using Pd(PPh₃)₄ as the catalyst. Finally, the target molecules were obtained by the Knoevenagel condensation reaction in a high yield (>90%). Although the two small molecules had a large core, they showed very good solubility in common organic solvents, such as tetrahydrofuran, chloroform, and chlorobenzene, which ensured their solution processability. The detailed synthesis procedures of the monomers are described in the Experimental Section.

The optical properties of NDTT-CNCOO and NDTP-CNCOO were investigated by UV-vis absorption spectra in both chloroform solution and thin films (Figure 1). In solution, the maximum absorption peaks and absorption edges of the two molecules were almost identical. From solution to solid state, both of them exhibited very obvious red-shifted absorption peaks and vibronic shoulder peaks, suggesting the molecule takes a rather planar structure and the existence of

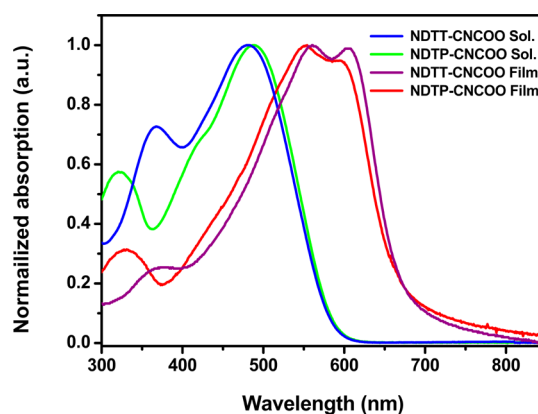


Figure 1. UV-vis absorption spectra of NDTT-CNCOO and NDTP-CNCOO in 1×10^{-5} M chloroform solution and at solid state.

Table 1. Optimal Data of NDTT-CNCOO/PC₇₁BM-Based Device and Photovoltaic Properties of NDTP-CNCOO/PC₇₁BM-Based BHJ Solar Cells Fabricated with Different Active Layer Thicknesses^a

small molecule	V_{oc} [V]	J_{sc} [mA/cm ²]	FF [%]	PCE [%]	thickness [nm]
NDTT-CNCOO	0.91 (0.91 ± 0.01)	7.40 (7.44 ± 0.14)	69.9 (68.7 ± 1.4)	4.71 (4.68 ± 0.05)	175 ± 5
NDTP-CNCOO	0.94 (0.94 ± 0.01)	7.72 (7.56 ± 0.16)	70.7 (70.3 ± 0.4)	5.13 (4.98 ± 0.15)	105 ± 7
	0.94 (0.94 ± 0.01)	8.01 (8.11 ± 0.10)	72.3 (70.8 ± 1.5)	5.44 (5.39 ± 0.08)	166 ± 6
	0.94 (0.94 ± 0.01)	8.99 (8.96 ± 0.07)	72.1 (72.0 ± 0.4)	6.09 (6.04 ± 0.07)	204 ± 8
	0.94 (0.94 ± 0.01)	9.98 (10.04 ± 0.07)	71.6 (70.6 ± 1.1)	6.71 (6.63 ± 0.10)	243 ± 9
	0.94 (0.94 ± 0.01)	10.77 (10.64 ± 0.22)	71.1 (71.6 ± 1.8)	7.20 (7.12 ± 0.10)	302 ± 6
	0.94 (0.94 ± 0.01)	10.49 (10.33 ± 0.16)	68.0 (68.5 ± 0.9)	6.70 (6.59 ± 0.11)	356 ± 8
	0.93 (0.93 ± 0.01)	10.37 (10.57 ± 0.20)	64.7 (63.6 ± 1.2)	6.24 (6.13 ± 0.11)	413 ± 8

^aThe effective areas of cells were 4 mm².

strong intermolecular π - π stacking interactions.²⁷ However, the shoulder peak intensity of NDTT-CNCOO was slightly stronger than that of NDTP-CNCOO, which indicated the increased degree of molecular aggregation. The optical band gap of NDTT-CNCOO was calculated from the film absorption edge as 1.85 eV, which is a little smaller than that of NDTP-CNCOO (1.88 eV). The electrochemical properties of NDTT-CNCOO and NDTP-CNCOO were measured by cyclic voltammetry (CV). The HOMO and lowest unoccupied molecular orbital levels were calculated from the onset oxidation and reduction potential (Figure S1) as -5.16 eV/-3.48 eV for NDTT-CNCOO and -5.18 eV/-3.45 eV for NDTP-CNCOO. The HOMO level of NDTP-CNCOO was deeper than that of NDTT-CNCOO and those of reported donor materials,²⁸ which would enable the corresponding photovoltaic device to exhibit high V_{oc} value.²⁹

The photovoltaic properties of two small molecules were explored by fabricating BHJ solar cells with a conventional structure of ITO/PEDOT:PSS/molecule:PC₇₁BM (w/w)/Ca/Al. According to the common practice for processing the analogous small molecules and their own good solubility in chloroform, chloroform was chosen as the spin-coating solvent.³⁰

For the NDTT-CNCOO-based device, the optimal D/A ratio was 1:0.5 (w/w) (Table S1). Different additives, such as 1,8-diiodooctane (DIO), 1-chloronaphthalene (CN), and diphenyl ether (DPE), were then added to improve device performance. The PCE of the NDTT-CNCOO-based device increased from 2.27% (without additive) to 4.32% by adding a very small amount of DPE (0.5%, v/v) (Table S2). Finally, the active layer thickness did not have much influence on the device performance, and a slightly better PCE of 4.71% was acquired with a short circuit current density (J_{sc}) of 7.40 mA cm⁻², V_{oc} of 0.91 V, and FF of 69.9% (Table S3).

Compared with NDTT-CNCOO, NDTP-CNCOO/PC₇₁BM-based BHJ solar cells exhibited much better performance at the donor/acceptor ratio (w/w) of 1:0.5 with 1.2% DIO (v/v) as the additive (Tables S4 and S5). Under this condition, a PCE of 6.71% was obtained with J_{sc} of 9.98 mA cm⁻², V_{oc} of 0.94 V, and FF of 71.6%, whereas the corresponding active layer thickness was 250 nm. For a majority of donor materials, the best performances were normally obtained at the active layer thickness of ~100 nm.³¹ Therefore, thinner active layers were employed to optimize device performance in the follow-up tests. However, thinner films led to poorer PCEs because of the decrease in J_{sc} . The effect of thicker active layers on device performance was further investigated. The detailed performance data of NDTP-CNCOO/PC₇₁BM-based devices with different active layer thicknesses are summarized in Table 1. As

shown in this table, the V_{oc} values remained at a high voltage of 0.94 V, which could be attributed to the relatively low HOMO level of the small molecule. The J_{sc} values increased continuously as the active layer thickness increased from 100 to 300 nm because of the enhanced absorption, and the FF values were maintained above 70%. However, when the thickness was beyond 300 nm, the decrease in FF originating from the enhanced charge recombination because of an increase in carrier drift length caused a significant reduction in PCE (Figure 2a).¹⁶ Thus, the highest PCE of 7.20% was finally observed with an active layer thickness of 300 nm (Figure 2b) and the PCEs all remained above 6.0% when the film thickness ranged from 200 to 400 nm. To date, this value is

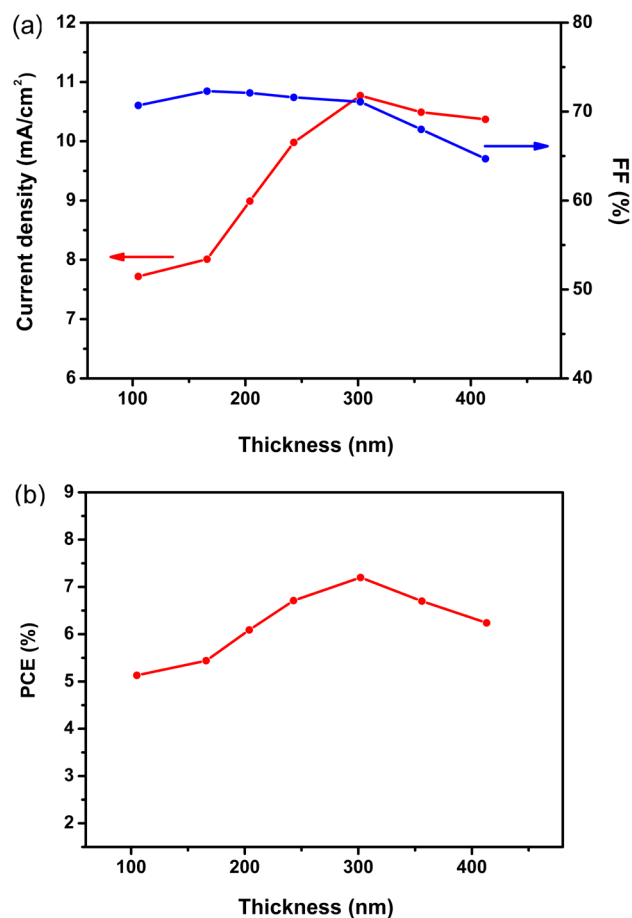


Figure 2. Plot of trends of J_{sc} /FF (a) and PCEs (b) with the active layer thickness for NDTP-CNCOO-based BHJ solar cells.

the best PCE reported for small molecule BHJ solar cells based on the NDT unit.

The best current–voltage (J – V) and external quantum efficiency (EQE) curves for the two small molecule-based devices are shown in Figure 3. The EQE curve of NDTP-

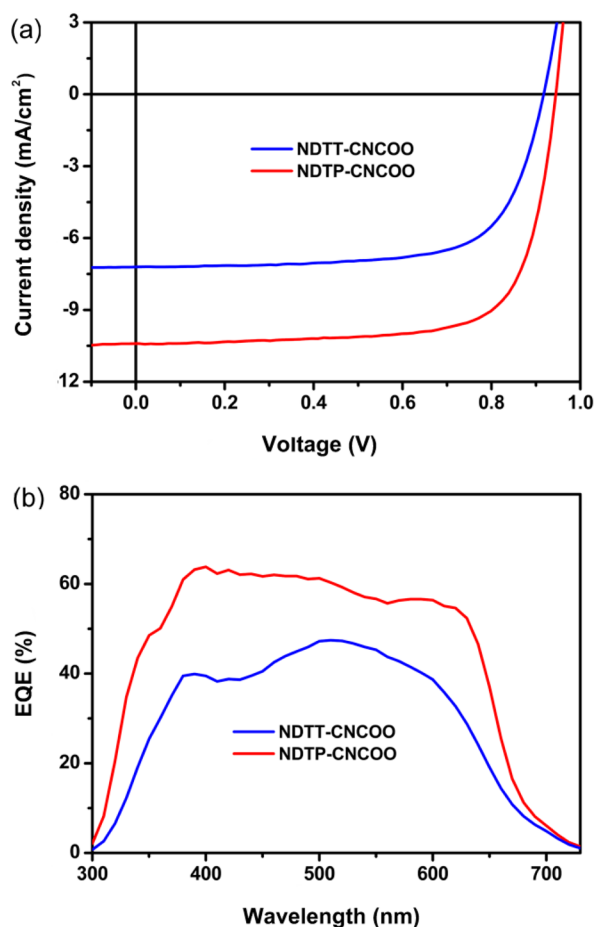


Figure 3. (a) J – V curves of two small molecule-based BHJ solar cells prepared under optimal conditions (D/A ratio = 1:0.5, 0.5% DPE, thickness = 175 ± 5 nm for NDTT-CNCOO; D/A ratio = 1:0.5, 1.2% DIO, thickness = 302 ± 6 nm for NDTP-CNCOO). (b) EQE curves of the corresponding device.

CNCOO exhibited a stronger photoresponse in the range of 380–520 nm with EQE values exceeding 60%, whereas the maximal EQE of NDTT-CNCOO was below 50% (Figure 3b). The J_{sc} value calculated from integration of the EQE curve was 7.07 mA cm^{-2} for NDTT-CNCOO and 10.27 mA cm^{-2} for NDTP-CNCOO, which showed around 4% mismatch compared with the J_{sc} value obtained from the J – V measurement.

The hole mobilities of the NDTT-CNCOO/PC₇₁BM and NDTP-CNCOO/PC₇₁BM blend film with an optimal active layer thickness were measured by the space-charge limited current (SCLC) method with a device structure of ITO/PEDOT:PSS/small molecule:PC₇₁BM/Au (Figure S2). The hole mobility of the NDTT-CNCOO/PC₇₁BM blend film (~ 180 nm) was $2.44 \times 10^{-4} \text{ cm}^2 \text{ V}^{-1} \text{ s}^{-1}$, whereas the NDTP-CNCOO/PC₇₁BM blend film (~ 300 nm) exhibited a relatively high hole mobility of $3.81 \times 10^{-4} \text{ cm}^2 \text{ V}^{-1} \text{ s}^{-1}$. Both films had the same order of magnitude as those of highly efficient small molecule donor materials.^{5,32} Such high hole mobilities even

with thick active layers could partially account for the high FFs of NDT-based small molecule solar cells, which was similar to another thick-film small molecule system reported by Chen and co-workers.¹⁴

Grazing-incidence wide-angle X-ray scattering (GIWAXS) analysis of the optimal NDTP-CNCOO/PC₇₁BM and NDTT-CNCOO/PC₇₁BM blend films was used to gain deeper insight into the crystallinity and molecular stacking mode of the two small molecules in the active layers. As shown in Figure 4, both blend films showed a conspicuous first-order diffraction peak ($100, q_{xy} \approx 0.3 \text{ \AA}^{-1}$), second-order diffraction peak ($200, q_{xy} \approx 0.6 \text{ \AA}^{-1}$), and third-order diffraction peak ($300, q_{xy} \approx 0.9 \text{ \AA}^{-1}$) in the out-of-plane direction, indicating the extremely highly ordered structure and superior crystallization capability of small molecules blended with PC₇₁BM. The calculated corresponding π – π stacking distances according to the diffraction peak (010) appearing along the q_{xy} axis for the two small molecules were 3.6 \AA , which was smaller than those of other high-performance donor small molecules (3.7 \AA).^{5,13} Such short π – π stacking distance between small molecule backbones suggested strong intermolecular interactions, which could promote efficient charge transport and lead to a higher FF.³³ Despite these similarities, some slight differences between the two small molecules were observed. On the one hand, as the diffraction peak (010) corresponding to π – π stacking predominantly appeared along the q_{xy} axis, both small molecules preferentially adopted the edge-on orientation in the blend film. However, NDTP-CNCOO still showed a diffraction (010) peak in the out-of-plane direction (Figure 4d) compared with NDTT-CNCOO. Although the diffraction peak intensity was slightly weak, it indicated a face-on orientation for NDTP-CNCOO, which was desirable to obtain a high J_{sc} and PCE for the corresponding photovoltaic device. This point can be confirmed by analyzing the pole figures extracted from the lamellar diffraction (100) in the GIWAXS patterns for the two blend films (Figure S3).¹¹ The ratio of face-on to edge-on for the NDTP-CNCOO/PC₇₁BM blend film was 0.194, which was higher than that for the NDTT-CNCOO/PC₇₁BM blend film (0.054). It is clear that the population of the face-on crystallite is larger in the NDTP-CNCOO/PC₇₁BM blend film than in the NDTT-CNCOO/PC₇₁BM blend film. On the other hand, NDTT-CNCOO exhibited slightly stronger crystallization capability than NDTP-CNCOO, suggesting that the former was more likely to aggregate and form larger domains in the blend film. Once this sort of aggregation behavior could not be tuned effectively during active layer preparation, the resulting large-scale phase separation would ultimately lead to poor device performance.

The morphologies of the two optimal active layers were investigated by atomic force microscopy (AFM) and transmission electron microscopy (TEM) analyses. AFM phase image (Figure 5a) of the NDTT-CNCOO/PC₇₁BM blend film revealed large-scale phase separation in the active layer. Meanwhile, the TEM image (Figure 5b) showed the existence of both small molecule and PC₇₁BM aggregations with a size of hundreds of nanometers. Such poor film morphology would dramatically suppress exciton diffusion and influence subsequent charge separation, resulting in low J_{sc} and poor PCE. As shown in the AFM phase image (Figure 5c) of the NDTP-CNCOO/PC₇₁BM blend film, the domain size was much smaller and phase separation was much better than that of the NDTT-CNCOO/PC₇₁BM blend film. On the basis of the corresponding TEM image (Figure 5d), PC₇₁BM was well

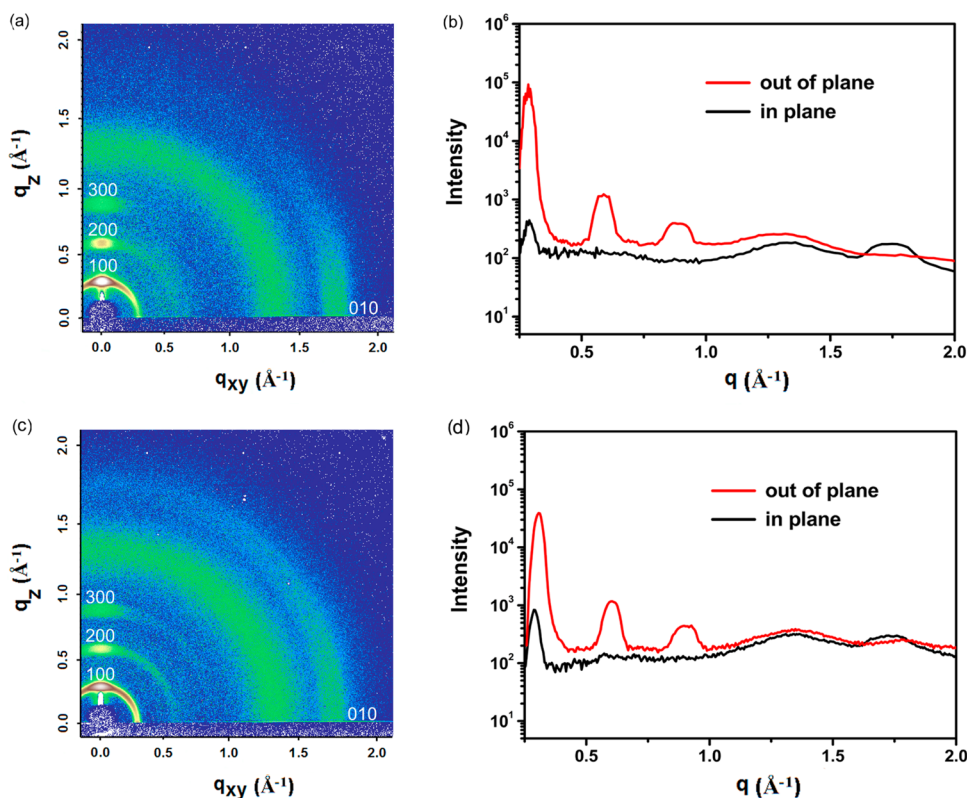


Figure 4. (a) GIWAXS image of the NDTP-CNCOO/PC₇₁BM blend film prepared under optimal conditions (D/A ratio = 1:0.5, 0.5% DPE, thickness = 175 ± 5 nm). (b) Out-of-plane and in-plane patterns of the corresponding film. (c) GIWAXS image of the NDTP-CNCOO/PC₇₁BM blend film prepared under optimal conditions (D/A ratio = 1:0.5, 1.2% DIO, thickness = 302 ± 6 nm). (d) Out-of-plane and in-plane patterns of the corresponding film.

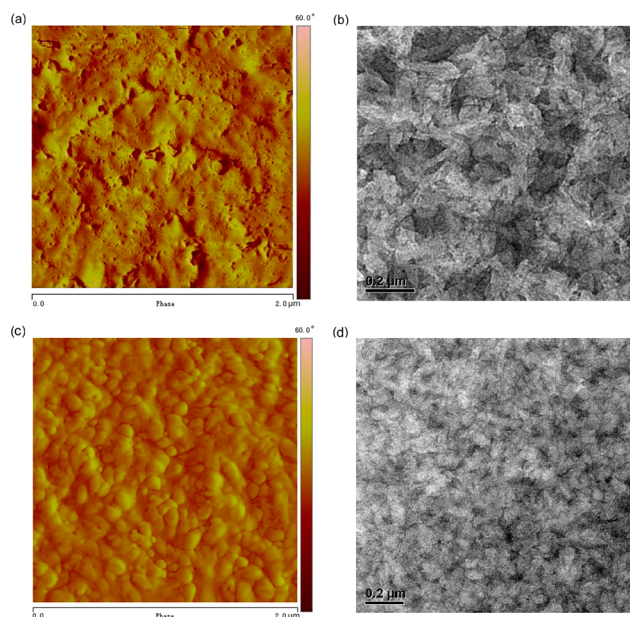


Figure 5. (a) AFM phase image of the NDTP-CNCOO/PC₇₁BM blend film prepared under optimal conditions. (b) TEM image of the same blend film. (c) AFM phase image of the NDTP-CNCOO/PC₇₁BM blend film prepared under optimal conditions. (d) TEM image of the same blend film. The size of the AFM image is 2.0 μm × 2.0 μm. The bar in the TEM image represents 200 nm.

dispersed around the small-molecule aggregates, which were derived from molecular packing. Such optimized morphology

with interpenetration of the donor and acceptor phases could enhance the efficiency of exciton diffusion and charge separation.³⁴ Furthermore, the ordered packing of NDTP-CNCOO could facilitate charge carrier transport. Therefore, a much higher J_{sc} and good performance were achieved for the NDTP-CNCOO/PC₇₁BM-based BHJ solar cell.

CONCLUSIONS

In summary, two novel small molecules (NDTP-CNCOO and NDTP-CNCOO) using 2D-conjugated NDT unit as the core were synthesized and fully characterized. As expected, an extremely highly ordered structure and excellent charge transport property were obtained by introducing a 2D-conjugated NDT unit to the small molecules because of the enhanced intermolecular π - π interactions. Compared with NDTP-CNCOO, NDTP-CNCOO/PC₇₁BM-based BHJ solar cells exhibited high FFs and PCEs even with thick active layers. Such performance benefitted from highly ordered structures, excellent charge transport property, and good film formation capability. More specifically, the FFs of solar cell devices were all above 70% with thicknesses of active layers ranging from 100 to 300 nm. The PCEs were all above 6.0% with a film thickness of 200–400 nm, and the optimal PCE reached 7.2% with an active layer thickness of 300 nm, which is the highest efficiency for small molecule BHJ solar cells based on the NDT unit to date. These results demonstrated that a 2D-conjugated NDT core was a very effective building block for the design of novel highly efficient small molecules applied in thick-film BHJ solar cells. Further optimization of the molecular structure on this

system is currently in progress to obtain better photovoltaic performance.

EXPERIMENTAL SECTION

Materials and Synthesis. Solvents and other common reagents were obtained from Beijing Chemical Plant. All other chemicals were purchased from commercial sources (Alfa, Acros, and Sigma–Aldrich) and used without further purification unless otherwise stated. THF, toluene, and chloroform were freshly distilled from appropriate drying agents prior to use. The detailed synthetic processes of NDTP are illustrated in the [Supporting Information](#).

NDTT-CHO. NDTT (478 mg, 0.5 mmol) and 3T-CHO (1.16 g, 2 mmol) were dissolved into anhydrous toluene (20 mL) in a three-neck flask. The solution was flushed with argon for 20 min, and Pd(PPh₃)₄ (25 mg) was added into the flask. The flask was subjected to three successive cycles of vacuum followed by refilling with argon. Polymerization was carried out at 100 °C for 48 h under argon protection. After cooling to room temperature, the reaction mixture was poured into water and extracted several times with dichloromethane. The organic phases were combined, washed with brine, and dried over anhydrous magnesium sulfate. The solvent was removed under reduced pressure, and the crude product was purified by column chromatography to yield NDTT-CHO as a red solid (520 mg, 64%). MS (MALDI-TOF): *m/z* = 1625.9. ¹H NMR (400 MHz, CDCl₃, ppm, δ): 9.80 (s, 2H), 7.89 (s, 2H), 7.82 (s, 2H), 7.56 (s, 2H), 7.28 (d, 2H), 7.21 (d, 2H), 7.13 (s, 2H), 7.09 (d, 2H), 6.91 (d, 2H), 2.90 (d, 4H), 2.82 (m, 8H), 1.71 (m, 14H), 1.32 (m, 52H), 1.01 (m, 12H), 0.89 (m, 12H).

NDTT-CNCOO. Two drops of trimethylamine and octyl cyanoacetate (630 mg, 3.2 mmol) were added to a solution of NDTT-CHO (520 mg, 0.32 mmol) in dry CHCl₃ (20 mL). The resulting solution was refluxed and stirred for 12 h under argon. After cooling to room temperature, the reaction mixture was poured into water and extracted several times with dichloromethane. The organic phases were combined, washed with brine, and dried over anhydrous magnesium sulfate. The solvent was removed under reduced pressure, and the crude product was purified by column chromatography for five times to yield NDTT-CNCOO as a black solid (590 mg, 93%). MS (MALDI-TOF): *m/z* = 1983.9. ¹H NMR (400 MHz, CDCl₃, ppm, δ): 8.17 (s, 2H), 7.91 (s, 2H), 7.85 (s, 2H), 7.57 (s, 2H), 7.31 (d, 2H), 7.28 (d, 2H), 7.15 (s, 2H), 7.12 (d, 2H), 6.92 (d, 2H), 4.29 (t, 4H), 2.90 (d, 4H), 2.84 (m, 8H), 1.74 (m, 14H), 1.33 (m, 76H), 1.01 (m, 12H), 0.89 (m, 18H). ¹³C NMR (100 MHz, CDCl₃, δ): 163.08, 145.68, 145.47, 141.74, 140.92, 140.70, 140.22, 139.73, 138.42, 138.27, 136.35, 135.93, 135.57, 134.08, 132.70, 130.01, 129.31, 128.00, 127.82, 126.28, 126.03, 125.85, 124.84, 116.02, 97.44, 66.53, 41.54, 34.35, 32.54, 31.97, 31.91, 31.81, 30.38, 30.13, 29.90, 29.80, 29.72, 29.64, 29.57, 29.53, 29.49, 29.39, 29.33, 29.23, 29.20, 28.99, 28.59, 25.84, 25.65, 23.14, 22.74, 22.71, 22.67, 14.26, 14.16, 14.14, 14.12, 10.94. Anal. Calcd for C₁₁₈H₁₅₄N₂O₄S₁₀: C, 71.39; H, 7.82; N, 1.41. Found: C, 71.64; H, 8.12; N, 1.32.

NDTP-CHO. NDTP (472 mg, 0.5 mmol) and 3T-CHO (1.16 g, 2 mmol) were dissolved into anhydrous toluene (20 mL) in a three-neck flask. The solution was flushed with argon for 20 min, and Pd(PPh₃)₄ (25 mg) was added into the flask. The flask was subjected to three successive cycles of vacuum followed by refilling with argon. Polymerization was carried out at 100 °C for 48 h under argon protection. After cooling to room temperature, the reaction mixture was poured into water and extracted several times with dichloromethane. The organic phases were combined, washed with brine, and dried over anhydrous magnesium sulfate. The solvent was removed under reduced pressure, and the crude product was purified by column chromatography to yield compound 7 as a red solid (452 mg, 56%). MS (MALDI-TOF): *m/z* = 1614.6. ¹H NMR (400 MHz, CDCl₃, ppm, δ): 9.84 (s, 2H), 7.92 (s, 2H), 7.64 (s, 2H), 7.63 (d, 4H), 7.60 (s, 2H), 7.38 (d, 4H), 7.30 (d, 2H), 7.19 (s, 2H), 7.15 (d, 2H), 2.85 (m, 8H), 2.69 (d, 4H), 1.72 (m, 14H), 1.27 (m, 52H), 0.98 (m, 12H), 0.89 (m, 12H).

NDTP-CNCOO. Two drops of trimethylamine and octyl cyanoacetate (552 mg, 2.8 mmol) were added to a solution of NDTP-CHO (452 mg, 0.28 mmol) in dry CHCl₃ (20 mL). The resulting solution was refluxed and stirred for 12 h under argon. After cooling to room temperature, the reaction mixture was poured into water and extracted several times with dichloromethane. The organic phases were combined, washed with brine, and dried over anhydrous magnesium sulfate. The solvent was removed under reduced pressure, and the crude product was purified by column chromatography for five times to yield NDTP-CNCOO as a black solid (522 mg, 94%). MS (MALDI-TOF): *m/z* = 1971.8. ¹H NMR (400 MHz, CDCl₃, ppm, δ): 8.19 (s, 2H), 7.91 (s, 2H), 7.64 (d, 4H), 7.61 (s, 2H), 7.59 (s, 2H), 7.38 (d, 4H), 7.30 (d, 2H), 7.17 (s, 2H), 7.14 (d, 2H), 4.30 (m, 4H), 2.85 (m, 8H), 2.69 (d, 4H), 1.75 (m, 2H), 1.70 (m, 12H), 1.27 (m, 76H), 0.98 (m, 12H), 0.89 (m, 18H). ¹³C NMR (100 MHz, CDCl₃, δ): 163.10, 145.82, 141.72, 141.64, 141.16, 140.70, 140.44, 138.40, 138.27, 137.66, 137.27, 136.65, 135.81, 134.20, 132.89, 129.88, 129.61, 128.94, 128.17, 127.84, 126.14, 125.19, 121.25, 120.80, 116.01, 97.67, 66.56, 41.16, 39.99, 32.46, 31.92, 31.88, 31.80, 30.43, 30.20, 29.68, 29.57, 29.50, 29.43, 29.32, 29.28, 29.21, 29.18, 28.94, 28.58, 25.82, 25.54, 23.13, 22.71, 22.69, 22.66, 14.24, 14.14, 14.12, 14.11, 10.88. Anal. Calcd for C₁₂₂H₁₅₈N₂O₄S₈: C, 74.26; H, 8.07; N, 1.42. Found: C, 74.12; H, 8.21; N, 1.29.

Measurements. Mass spectra were determined on a Bruker microflex MALDI-TOF mass spectrometer. ¹H NMR (400 MHz) was obtained on a Bruker Avance 400 NMR spectrometer using tetramethylsilane as an internal standard. UV–vis absorption spectra were recorded on a Shimadzu UV-3600 UV–vis–NIR spectrophotometer. Electrochemical CV was conducted on an EG&G Princeton Applied Research VMP3 workstation with Pt disk coated with the polymer film, Pt plate, and Ag/Ag⁺ electrode as the working electrode, counter electrode, and reference electrode, respectively, in a 0.1 mol/L tetrabutylammoniumhexafluorophosphate (Bu₄NPF₆) acetonitrile solution. The *J*–*V* curves were obtained by a Keithley 2420 source measure unit. The photocurrent was measured under illumination using an Oriel Newport 150W solar simulator (AM 1.5G), and the light intensity was calibrated with a Newport reference detector (Oriel PN 91150 V). The EQE measurements of the devices were performed in air with an Oriel Newport system (Model 66902). The thickness of the active layer was measured on a Kla-Tencor Alpha-Step D-120 Stylus Profiler. AFM images were obtained on a Nanoscope IIIa AFM Multimode Digital Instrument in tapping mode. TEM measurements were performed on a Tecnai G2 F20 U-TWIN instrument under proper defocus conditions. GIWAXS experiments were conducted using XEUS SAXS/WAXS equipment.

ASSOCIATED CONTENT

Supporting Information

The Supporting Information is available free of charge on the [ACS Publications website](#) at DOI: [10.1021/acs.chemmater.5b04668](https://doi.org/10.1021/acs.chemmater.5b04668).

Experimental section, ¹H NMR spectra, ¹³C NMR spectra, mass spectra, CV curves, *J*–*V* characteristics of SCLC, and other device data. ([PDF](#))

AUTHOR INFORMATION

Corresponding Authors

*E-mail: weizx@nanoctr.cn.

*E-mail: lvk@nanoctr.cn.

Notes

The authors declare no competing financial interest.

ACKNOWLEDGMENTS

This work was supported by the National Natural Science Foundation of China (Grant Nos. 21125420 and 21474022), the Beijing Municipal Science and Technology Commission

(Nos. Z141100003814010 and D151100003315002), and the Chinese Academy of Sciences.

REFERENCES

- (1) Ni, W.; Wan, X. J.; Li, M. M.; Wang, Y. C.; Chen, Y. S. A-D-A small molecules for solution-processed organic photovoltaic cells. *Chem. Commun.* **2015**, *51*, 4936–4950.
- (2) Liu, Y.; Wan, X.; Wang, F.; Zhou, J.; Long, G.; Tian, J.; You, J.; Yang, Y.; Chen, Y. Spin-coated small molecules for high performance solar cells. *Adv. Energy Mater.* **2011**, *1*, 771–775.
- (3) Li, M.; Ni, W.; Wan, X.; Zhang, Q.; Kan, B.; Chen, Y. Benzo[1,2-*b*:4,5-*b'*]dithiophene (BDT)-based small molecules for solution processed organic solar cells. *J. Mater. Chem. A* **2015**, *3*, 4765–4776.
- (4) Liu, Y.; Chen, C.-C.; Hong, Z.; Gao, J.; Yang, Y.; Zhou, H.; Dou, L.; Li, G.; Yang, Y. Solution-processed small-molecule solar cells: breaking the 10% power conversion efficiency. *Sci. Rep.* **2013**, *3*, 3356–3363.
- (5) Kan, B.; Li, M.; Zhang, Q.; Liu, F.; Wan, X.; Wang, Y.; Ni, W.; Long, G.; Yang, X.; Feng, H.; Zuo, Y.; Zhang, M.; Huang, F.; Cao, Y.; Russell, T. P.; Chen, Y. A series of simple oligomer-like small molecules based on oligothiophenes for solution-processed solar cells with high efficiency. *J. Am. Chem. Soc.* **2015**, *137*, 3886–3893.
- (6) Li, W. W.; Hendriks, K. H.; Roelofs, W. S. C.; Kim, Y.; Wienk, M. M.; Janssen, R. A. J. Efficient small bandgap polymer solar cells with high fill factors for 300 nm thick films. *Adv. Mater.* **2013**, *25*, 3182–3186.
- (7) Hu, X.; Yi, C.; Wang, M.; Hsu, C.-H.; Liu, S.; Zhang, K.; Zhong, C.; Huang, F.; Gong, X.; Cao, Y. High-performance inverted organic photovoltaics with over 1 μm thick active layers. *Adv. Energy Mater.* **2014**, *4*, 1400378–1400385.
- (8) Nguyen, T. L.; Choi, H.; Ko, S. J.; Uddin, M. A.; Walker, B.; Yum, S.; Jeong, J. E.; Yun, M. H.; Shin, T. J.; Hwang, S.; Kim, J. Y.; Woo, H. Y. Semi-crystalline photovoltaic polymers with efficiency exceeding 9% in a ~ 300 nm thick conventional single-cell device. *Energy Environ. Sci.* **2014**, *7*, 3040–3051.
- (9) Liu, Y.; Zhao, J.; Li, Z.; Mu, C.; Ma, W.; Hu, H.; Jiang, K.; Lin, H.; Ade, H.; Yan, H. Aggregation and morphology control enables multiple cases of high-efficiency polymer solar cells. *Nat. Commun.* **2014**, *5*, 5293–5300.
- (10) Choi, H.; Ko, S.-J.; Kim, T.; Morin, P.-O.; Walker, B.; Lee, B. H.; Leclerc, M.; Kim, J. Y.; Heeger, A. J. Small-bandgap polymer solar cells with unprecedented short-circuit current density and high fill factor. *Adv. Mater.* **2015**, *27*, 3318–3324.
- (11) Vohra, V.; Kawashima, K.; Kakara, T.; Koganezawa, T.; Osaka, I.; Takimiya, K.; Murata, H. Efficient inverted polymer solar cells employing favourable molecular orientation. *Nat. Photonics* **2015**, *9*, 403–408.
- (12) Li, W.; Yan, L.; Zhou, H.; You, W. A general approach toward electron deficient triazole units to construct conjugated polymers for solar cells. *Chem. Mater.* **2015**, *27*, 6470–6476.
- (13) Sun, K.; Xiao, Z.; Lu, S.; Zajaczkowski, W.; Pisula, W.; Hanssen, E.; White, J. M.; Williamson, R. M.; Subbiah, J.; Ouyang, J.; Holmes, A. B.; Wong, W. W. H.; Jones, D. J. A molecular nematic liquid crystalline material for high-performance organic photovoltaics. *Nat. Commun.* **2015**, *6*, 6013–6021.
- (14) Zhang, Q.; Kan, B.; Wan, X.; Zhang, H.; Liu, F.; Li, M.; Yang, X.; Wang, Y.; Ni, W.; Russell, T. P.; Shen, Y.; Chen, Y. Large active layer thickness toleration of high-efficiency small molecule solar cells. *J. Mater. Chem. A* **2015**, *3*, 22274–22279.
- (15) Cui, C.; Guo, X.; Min, J.; Guo, B.; Cheng, X.; Zhang, M.; Brabec, C. J.; Li, Y. High-performance organic solar cells based on a small molecule with alkythio-thienyl-conjugated side chains without extra treatments. *Adv. Mater.* **2015**, *27*, 7469.
- (16) Lenes, M.; Koster, L. J. A.; Mihailitchi, V. D.; Blom, P. W. M. Thickness dependence of the efficiency of polymer:fullerene bulk heterojunction solar cells. *Appl. Phys. Lett.* **2006**, *88*, 243502–243504.
- (17) Yang, H.; Shin, T. J.; Yang, L.; Cho, K.; Ryu, C. Y.; Bao, Z. Effect of mesoscale crystalline structure on the field-effect mobility of regioregular poly(3-hexyl thiophene) in thin-film transistors. *Adv. Funct. Mater.* **2005**, *15*, 671–676.
- (18) Zhu, X. W.; Fang, J.; Lu, K.; Zhang, J. Q.; Zhu, L. Y.; Zhao, Y. F.; Shuai, Z. G.; Wei, Z. X. Naphtho[1,2-*b*:5,6-*b'*]dithiophene based two-dimensional conjugated polymers for highly efficient thick-film inverted polymer solar cells. *Chem. Mater.* **2014**, *26*, 6947–6954.
- (19) Dutta, P.; Yang, W.; Lee, W. H.; Kang, I. N.; Lee, S. H. Novel naphtho[1,2-*b*:5,6-*b'*]dithiophene core linear donor- π -acceptor conjugated small molecules with thiophene-bridged bithiazole acceptor: design, synthesis, and their application in bulk heterojunction organic solar cells. *J. Mater. Chem.* **2012**, *22*, 10840–10851.
- (20) Dutta, P.; Yang, W.; Eom, S. H.; Lee, W.-H.; Kang, I. N.; Lee, S.-H. Development of naphtho[1,2-*b*:5,6-*b'*]dithiophene based novel small molecules for efficient bulk-heterojunction organic solar cells. *Chem. Commun.* **2012**, *48*, 573–575.
- (21) Loser, S.; Miyauchi, H.; Hennek, J. W.; Smith, J.; Huang, C.; Facchetti, A.; Marks, T. J. A "zig-zag" naphthodithiophene core for increased efficiency in solution-processed small molecule solar cells. *Chem. Commun.* **2012**, *48*, 8511–8514.
- (22) Dou, L. T.; Gao, J.; Richard, E.; You, J. B.; Chen, C. C.; Cha, K. C.; He, Y. J.; Li, G.; Yang, Y. Systematic investigation of benzodithiophene- and diketopyrrolopyrrole-based low-bandgap polymers designed for single junction and tandem polymer solar cells. *J. Am. Chem. Soc.* **2012**, *134*, 10071–10079.
- (23) Zhang, M. J.; Gu, Y.; Guo, X.; Liu, F.; Zhang, S. Q.; Huo, L. J.; Russell, T. P.; Hou, J. H. Efficient polymer solar cells based on benzothiadiazole and alkylphenyl substituted benzodithiophene with a power conversion efficiency over 8%. *Adv. Mater.* **2013**, *25*, 4944–4949.
- (24) Shi, S. W.; Shi, K. L.; Qu, R.; Mao, Z. P.; Wang, H. L.; Yu, G.; Li, X. Y.; Li, Y. F.; Wang, H. Q. Alkylphenyl substituted naphthodithiophene: a new building unit with conjugated side chains for semiconducting materials. *Macromol. Rapid Commun.* **2014**, *35*, 1886–1889.
- (25) Shinamura, S.; Sugimoto, R.; Yanai, N.; Takemura, N.; Kashiki, T.; Osaka, I.; Miyazaki, E.; Takimiya, K. Orthogonally functionalized naphthodithiophenes: selective protection and borylation. *Org. Lett.* **2012**, *14*, 4718–4721.
- (26) Zhou, J.; Wan, X.; Liu, Y.; Long, G.; Wang, F.; Li, Z.; Zuo, Y.; Li, C.; Chen, Y. A planar small molecule with dithienosilole core for high efficiency solution-processed organic photovoltaic cells. *Chem. Mater.* **2011**, *23*, 4666–4668.
- (27) Lim, N.; Cho, N.; Paek, S.; Kim, C.; Lee, J. K.; Ko, J. High-Performance Organic Solar Cells with Efficient Semiconducting Small Molecules Containing an Electron-Rich Benzodithiophene Derivative. *Chem. Mater.* **2014**, *26*, 2283–2288.
- (28) Zhou, J.; Zuo, Y.; Wan, X.; Long, G.; Zhang, Q.; Ni, W.; Liu, Y.; Li, Z.; He, G.; Li, C.; Kan, B.; Li, M.; Chen, Y. Solution-processed and high-performance organic solar cells using small molecules with a benzodithiophene unit. *J. Am. Chem. Soc.* **2013**, *135*, 8484–8487.
- (29) Scharber, M. C.; Mühlbacher, D.; Koppe, M.; Denk, P.; Waldauf, C.; Heeger, A. J.; Brabec, C. J. Design rules for donors in bulk-heterojunction solar cells—towards 10% energy-conversion efficiency. *Adv. Mater.* **2006**, *18*, 789–794.
- (30) Zhou, J.; Wan, X.; Liu, Y.; Zuo, Y.; Li, Z.; He, G.; Long, G.; Ni, W.; Li, C.; Su, X.; Chen, Y. Small molecules based on benzo[1,2-*b*:4,5-*b'*]dithiophene unit for high-performance solution-processed organic solar cells. *J. Am. Chem. Soc.* **2012**, *134*, 16345–16351.
- (31) Kroon, R.; Diaz de Zerio Mendaza, A.; Himmelberger, S.; Bergqvist, J.; Bäcke, O.; Faria, G. C.; Gao, F.; Obaid, A.; Zhuang, W.; Gedefaw, D.; Olsson, E.; Inganäs, O.; Salteo, A.; Müller, C.; Andersson, M. R. A new tetracyclic lactam building block for thick, broad-bandgap photovoltaics. *J. Am. Chem. Soc.* **2014**, *136*, 11578–11581.
- (32) Kan, B.; Zhang, Q.; Li, M.; Wan, X.; Ni, W.; Long, G.; Wang, Y.; Yang, X.; Feng, H.; Chen, Y. Solution-processed organic solar cells based on dialkylthiol-substituted benzodithiophene unit with efficiency near 10%. *J. Am. Chem. Soc.* **2014**, *136*, 15529–15532.

(33) Guo, X.; Zhou, N.; Lou, S. J.; Smith, J.; Tice, D. B.; Hennek, J. W.; Ortiz, R. P.; Navarrete, J. T. L.; Li, S.; Strzalka, J.; Chen, L. X.; Chang, R. P. H.; Facchetti, A.; Marks, T. J. Polymer solar cells with enhanced fill factors. *Nat. Photonics* **2013**, *7*, 825–833.

(34) Mishra, A.; Bäuerle, P. Small molecule organic semiconductors on the move: promises for future solar energy technology. *Angew. Chem., Int. Ed.* **2012**, *51*, 2020–2067.